arXiv:nucl-th/0305020v3 25 Jun 2003

Electromagnetic response of confined Dirac particles

Mark W. Paris*

Theoretical Division, Los Alamos National Laboratory,

MS B283, Los Alamos, NM 87545 and

Departement für Physik und Astronomie, Universität Basel, Switzerland

(Dated: February 8, 2008)

Abstract

The eigenstates of a single massless Dirac particle confined in a linear potential are calculated exactly by direct solution of the Dirac equation. The electromagnetic structure functions are calculated from the Dirac wave functions of the ground and excited states of the particle by coupling to its conserved vector current. We obtain the longitudinal and transverse structure functions as a function of $\tilde{y} = \nu - |\mathbf{q}|$, where ν and $|\mathbf{q}|$ are the energy and momentum transferred to the target in its rest frame. At values of $|\mathbf{q}| \gtrsim 2.5$ GeV, much larger than the characteristic energy scale $\sim$ 440 MeV of the confining potential, the response exhibits $\tilde{y}$ scaling, a generalization of Bjorken scaling. We compare the exact structure functions with those obtained from the ground state wave functions in the plane wave impulse approximation. The deviation from the Callan-Gross relation is compared with the parton model prediction.

PACS numbers: 13.60.Hb,12.39.Ki,12.39.Pn

*paris@lanl.gov

I. INTRODUCTION

The present work is motivated by the study of the effects of interactions on the response of systems of confined relativistic particles. Here we consider a single massless Dirac particle confined by a linear potential. The Dirac Hamiltonian is solved exactly for a large number of eigenstates and the electromagnetic structure functions are calculated by coupling a charged leptonic probe (such as the electron) to the conserved vector current of the target, $\bar{\psi}_q(x)\gamma_\mu\psi_q(x)$. This model neglects some of the important physics such as the contribution of $q\bar{q}$ pairs from the vacuum and the effects of radiative gluon corrections. It is nevertheless useful to study the role of interactions on valence quark structure functions. In a future paper we will use this model to investigate the role of interactions in determining spin-dependent observables.[1]

The model may be viewed as a heavy-light meson, such as $\bar{t}u$, or a baryon with a light quark bound to an infinitely massive diquark. In the heavy-light meson, the antiquark $\bar{t}$ and light quark u have opposite color charge and confinement is due to the flux tube connecting them. In the limit of very large mass of the $\bar{t}$ the Dirac equation for the motion of the light quark is exact. We neglect the weak interaction.

Benhar, Pandharipande, and Sick [2] have shown that the transverse structure function of the proton $W_1^p(\tilde{y}, |\mathbf{q}|)$, measured in inclusive deep inelastic scattering (DIS) experiments, exhibits scaling in the variable $\tilde{y} = \nu - |\mathbf{q}|$ over a large range, 5 GeV $\leq |\mathbf{q}| \leq$ 100 GeV. Here ν and $|\mathbf{q}|$ are the energy and momentum transferred to the target in its rest frame. The model described in the present work also exhibits $\tilde{y}$ scaling. The $\tilde{y}$ variable is related to the dimensionless Nachtmann variable [3] $\xi = -\tilde{y}/M$, where M is the target mass. The variable $\tilde{y}$ is appropriate to systems where the constituents of the target move relativistically.[4] It and the Nachtmann ξ are generalizations [2, 5] of the Bjorken scaling variable x_B. Their relation is given by:

$$\xi = -\frac{\tilde{y}}{M} = \frac{2x_B}{1 + \sqrt{1 + \frac{4x_B^2 M^2}{Q^2}}}, \tag{1}$$

with $Q^2 = |\mathbf{q}|^2 - \nu^2$, giving $\xi = x_B$ in the limit $Q^2 \to \infty$.

In Ref.[5] we calculated the exact response of a single relativistic scalar "quark" confined by a linear potential. The response of this simple model exhibited a rich behavior and allowed the study of a diverse range of phenomena. We observed the $\tilde{y}$ scaling of the response in the

spacelike and timelike regions of momentum transfer, an approach to scaling qualitatively similar to the one found in recent inclusive experiments of DIS of electrons by proton [6], and Bloom-Gilman duality [7]. We also studied various approximations to the exact result. In particular the on-shell approximation (OSA), which assumes that constituents of a hadronic target are on the mass-shell before and after interaction with the probe, admits response only in the spacelike region of momentum transfer due to the inequality

$$\nu = \sqrt{|\mathbf{k}+\mathbf{q}|^2 + m^2} - \sqrt{|\mathbf{k}|^2 + m^2} \leqslant |\mathbf{q}|, \tag{2}$$

where $\mathbf{k}$ is the momentum of the struck constituent and m is its mass. In contrast, the plane wave impulse approximation (PWIA), often used in nuclear physics, treats the initial state constituents as bound particles, which are therefore not on their mass-shell, and Eq.(2) is not satisfied. Thus there is response in the timelike region in PWIA due to the bound nature of the constituents. Final state interactions (FSI), however, are neglected in PWIA and the state of the particle after it is struck by the probe is described as a plane wave.

In Ref.[4] we investigated the role of FSI effects on the response. There we found that FSI broadens the PWIA response, shifting more strength into the timelike region of momentum transfer. This broadening of the response due to FSI persists as $|\mathbf{q}| \to \infty$. The exact response was shown to be calculable by convolution of the PWIA response with a "folding function." This function describes the distribution in energy of a plane wave state in the linear confining well. It becomes independent of the three-momentum $|\mathbf{q}|$ transferred to the target in the limit of large $|\mathbf{q}|$ (*i.e.* the "scaling" limit). Thus the $\tilde{y}$ scaling, and equivalently Nachtmann ξ scaling or Bjorken scaling of the exact response is not a signal that FSI may be neglected. In fact, in the semi-relativistic model of Ref.[4] it is crucial to take into account FSI in order to reproduce the response *even in the scaling limit*, $|\mathbf{q}| \to \infty$. This situation is distinct from the case of a confining potential with a non-relativistic kinetic energy. In such a model, the width of the response scales linearly with $|\mathbf{q}|$. This precludes the need to take FSI into account in the scaling limit. It is also interesting to note that there is no Bloom-Gilman duality in the non-relativistic model. Since the width of the response scales linearly with $|\mathbf{q}|$ the resonant structure of the response at low-$|\mathbf{q}|$ does not average around the more broad response at high-$|\mathbf{q}|$.

The semi-relativistic model leaves much to be desired. Among its shortcomings are an ill-defined current operator, neglect of the contribution of $q\bar{q}$ pairs, and neglect of radiative

gluon effects. In this work we address the most egregious of these shortcomings by working with the conserved electromagnetic current of the confined particles, $\bar{\psi}_q(x)\gamma_\mu\psi_q(x)$.

We proceed by solving the Dirac equation for an assumed potential

$$V = V(r)\frac{1}{2}(1+\beta) = V(r)\begin{pmatrix} 1 & 0 \\ 0 & 0 \end{pmatrix} \tag{3}$$

$$V(r) = \sqrt{\sigma}r. \tag{4}$$

This potential has been investigated by Page, Ginocchio, and Goldman [8] and shown to admit a *spin symmetry* which suppresses spin-orbit coupling in the hadron spectrum. This symmetry results in the degeneracy of states with the same orbital angular momentum ℓ of the upper component of the Dirac wave function. The states with $j = \ell \pm \frac{1}{2}$ are degenerate and they have Dirac quantum numbers $\kappa = -(\ell+1)$ and ℓ, respectively. Recall that $\kappa = \pm(j+\frac{1}{2})$ where the upper (lower) sign is used when $j = \ell \mp \frac{1}{2}$. This potential is easy to work with since the lower components of the wave function are not coupled by the Dirac matrix of Eq.(3).

In the next section we will briefly detail the solution of the single particle Dirac equation for this potential. Section III gives the calculation of the electromagnetic structure functions. We discuss the interpretation of the contribution to the structure functions of the negative energy states. Section IV briefly compares the exact structure functions to those obtained in the PWIA. In the concluding Sec. V, we study the deviation from the Callan-Gross relation.

II. DIAGONALIZATION IN THE STATIC BAG MODEL BASIS

We wish to solve the Dirac equation

$$H\Psi^P_{n\kappa m} = \left[\boldsymbol{\alpha}\cdot\mathbf{p} + V\right]\Psi^P_{n\kappa m} = E^P_{n\kappa}\Psi^P_{n\kappa m} \tag{5}$$

for a massless fermion in the potential given in Eq.(3). Here n, κ, and m are the quantum numbers of a Dirac particle in a spherically symmetric potential. The Eq.(5) with potential given by Eqs.(3,4) has a discrete spectrum of bound positive energy $P = +$ states with wave functions that vanish as $r \to \infty$. However, due to the form of the Dirac matrix in Eq.(3) the wave functions of negative energy states are unbound.

We expand the eigenstates $\Psi^P_{n\kappa m}$ in a complete basis of static bag model (herein "bag model") states $\Phi^P_{\alpha\kappa m}$. (The explicit form of the bag model states $\Phi^P_{\alpha\kappa m}$ is given in the

Appendix A.) The expansion is

$$\Psi^P_{n\kappa m} = \sum_{\alpha=1,\ldots,\infty} [A^+_{n\kappa\alpha}\Phi^+_{\alpha\kappa m} + A^-_{n\kappa\alpha}\Phi^-_{\alpha(-\kappa)m}]. \tag{6}$$

Here we have explicitly written out the positive, $\Phi^+_{\alpha\kappa m}$ and negative, $\Phi^-_{\alpha(-\kappa)m}$ energy terms in the expansion of the eigenstates of H. The bag model states, $\Phi^P_{\alpha\kappa m}$ are eigenstates of $\mathcal{K} = \beta(\boldsymbol{\sigma}\cdot\mathbf{L}+1)$ with eigenvalue

$$\mathcal{K}\Phi^P_{\alpha\kappa m} = -\mathrm{sgn}\, P\kappa\Phi^P_{\alpha\kappa m}. \tag{7}$$

The potential mixes $P = +$ and $P = -$ bag model states with opposite signs of κ.

In the bag model basis the Dirac equation is

$$\sum_{P',P,\kappa',\kappa,\alpha',\alpha} \left[\langle\Phi^{P'}_{\alpha'\kappa' m}|V|\Phi^P_{\alpha\kappa m}\rangle + (E^P_{n\kappa} - \mathrm{sgn}PE_{\alpha\kappa})\delta_{P',P}\delta_{\kappa',\kappa}\delta_{\alpha',\alpha}\right] A^P_{n\kappa\alpha} = 0. \tag{8}$$

The non-zero terms appearing in potential matrix element have $(P',\kappa';P,\kappa) = (+,+;+,+),(+,+;-,-),(+,-;+,-),(-,+;-,+),(+,-;-,+)$, and $(-,-;-,-)$ and states obtained from these by $(P',\kappa') \leftrightarrow (P,\kappa)$.

The $E_{\alpha\kappa}$ are the eigenstates of the free Dirac Hamiltonian $E_{\alpha\kappa} = p_{\alpha\kappa}$ with momenta $p_{\alpha\kappa}$ fixed by the bag model boundary condition

$$\bar{\Phi}^+_{\alpha\kappa}(r)\Phi^+_{\alpha\kappa}(r)|_{r=R} = 0 \tag{9}$$

where $\bar{\Phi} = \Phi^\dagger\gamma^0$ and r is the bag radius. We consider only $\Phi^+_{\alpha\kappa}$ in Eq.(9) since the negative energy states yield the same momenta $p_{\alpha\kappa}$.

We solve Eq.(8) in the bag model basis up to some maximum value of the momentum $p_{\alpha_m\kappa}$. We include enough states in the basis so that the longitudinal sum rule, $S_L(|\mathbf{q}|)$ (see Eq.(25) of the next section) is satisfied. The value of the radius R is set by the requirement that radii of all included positive energy eigenstates of H have *rms* radii $\ll R$. $R = 15$ fm is used to satisfy this condition. The negative energy eigenstates have a continuum of eigenvalues in the limit $R \to \infty$ and therefore are R-dependent when R is finite.

The diagonalization of Eq.(8) is effected for each negative value of κ. The spin symmetry admitted by H allows one to obtain the states with $\kappa > 0$ from those with $\kappa < 0$ since the states with $\kappa + \kappa' = -1$ are degenerate. For each value of κ, angular integrations in the matrix elements of the potential in Eq.(8) are evaluated explicitly. H is then diagonalized

in a truncated basis of radial states (spherical Bessel functions appearing in the bag model states – see Appendix A) with wave numbers $\{p_{\alpha\kappa}\}_{\alpha=1}^{\alpha_m}$. In this work we take $\alpha_m = 600$. Thus for each κ we have 600 positive energy and 600 negative energy states in the basis.

The eigenstates of Eq.(5) can be written

$$\Psi^P_{n\kappa m} = \begin{pmatrix} f_{n\kappa}(r)\mathcal{Y}^\ell_{jm}(\hat{\mathbf{r}}) \\ ig_{n\kappa}(r)\mathcal{Y}^{\ell\pm1}_{jm}(\hat{\mathbf{r}}) \end{pmatrix} \tag{10}$$

where the angular part of the wave function is the spin-angle function, $\mathcal{Y}^\ell_{jm}$, with orbital angular momentum ℓ and spin-$\frac{1}{2}$ coupled to total angular momentum j and projection m. The upper (lower) sign in the angular part of the lower component of the wave function is taken when κ is negative (positive) with $\kappa = \ell > 0$ and $\kappa = -(\ell+1) < 0$. We obtain, from the expansion Eq.(6) and the explicit forms of the bag model wave functions Eqs.(A2) and (A3) and their negative energy counterparts, the expressions for the radial wave functions (for $\kappa < 0$)

$$f_{n\kappa}(r) = \sum_{\alpha=1}^{\alpha_m} \left(A^+_{n\kappa\alpha} N_{\alpha\kappa} j_\ell(p_{\alpha\kappa} r) - iA^-_{n(-\kappa)\alpha} N_{\alpha(-\kappa)} \sqrt{\frac{E_{\alpha(-\kappa)} - m}{E_{\alpha(-\kappa)} + m}} j_\ell(p_{\alpha(-\kappa)} r) \right) \tag{11}$$

$$g_{n\kappa}(r) = \sum_{\alpha=1}^{\alpha_m} \left(-A^+_{n\kappa\alpha} N_{\alpha\kappa} \sqrt{\frac{E_{\alpha\kappa} - m}{E_{\alpha\kappa} + m}} j_{\ell+1}(p_{\alpha\kappa} r) - iA^-_{n(-\kappa)\alpha} N_{\alpha(-\kappa)} j_{\ell+1}(p_{\alpha(-\kappa)} r) \right). \tag{12}$$

Analogous expressions hold for $\kappa > 0$.

We note that the ground state has energy $E_0 = 840$ MeV and *rms* radius $\langle r^2 \rangle^{\frac{1}{2}} = 0.66$ fm for string tension $\sqrt{\sigma} = 1$ GeV/fm. This string tension corresponds to a characteristic energy scale of $\sigma^{1/4} = 440$ MeV. On the basis of dimensional analysis we find that $E_0 \propto \sigma^{\frac{1}{4}}$.

III. ELECTROMAGNETIC STRUCTURE FUNCTIONS

The inclusive cross section for a spin-$\frac{1}{2}$ electromagnetic probe scattering from a hadronic target may be expressed to first order in the fine structure constant α as

$$\frac{d^2\sigma}{dE' d\Omega} = \sigma_M \left(W_2 + 2W_1 \tan^2(\theta/2) \right) \tag{13}$$

$$= \sigma_M \frac{Q^2}{|\mathbf{q}|^2} \left[W_L + W_T \left(1 + 2\frac{|\mathbf{q}|^2}{Q^2} \tan^2(\theta/2) \right) \right]. \tag{14}$$

Here σ_M is the Mott cross section

$$\sigma_M = \frac{\alpha_q^2 \cos^2(\theta/2)}{4E^2 \sin^4(\theta/2)}, \tag{15}$$

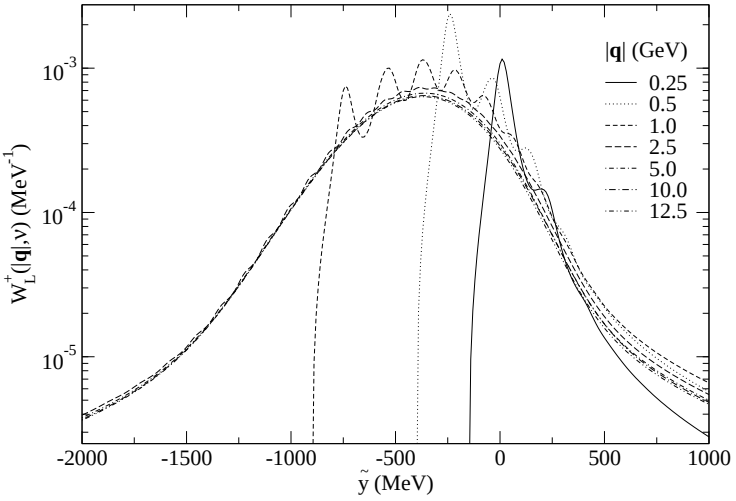

FIG. 1: The longitudinal structure function $W_L^+(|\mathbf{q}|,\nu)$ vs. $\tilde{y} = \nu - |\mathbf{q}|$ for various values of the three-momentum transfer.

with θ the probe's scattering angle, $E(E')$ its initial (final) energy and $\alpha_q = Q_q\alpha$, Q_q is the charge on the hadronic target's constituent in units of the proton's charge and α is the fine structure constant. We have neglected the mass of the electromagnetic probe in the above. The inclusive longitudinal, W_L and transverse, W_T structure functions are related to the functions $W_{1,2}$ by

$$W_T \;=\; W_1 \tag{16}$$

$$W_L \;=\; -W_1 + \frac{|\mathbf{q}|^2}{Q^2} W_2. \tag{17}$$

We have assumed that $q^\mu = (\nu, 0, 0, |\mathbf{q}|)$ and defined $Q^2 = -q^2 = |\mathbf{q}|^2 - \nu^2$.

The inclusive structure functions are determined from the matrix elements of the hadronic current on the target eigenstates and their energy eigenvalues as

$$W_L^+(|\mathbf{q}|,\nu) \;=\; \frac{1}{2}\sum_{m,I} \left|\langle I|\Lambda_+ e^{i\mathbf{q}\cdot\mathbf{r}}|0,m\rangle\right|^2 \delta(E_I - E_0 - \nu), \tag{18}$$

$$W_T^+(|\mathbf{q}|,\nu) \;=\; \frac{1}{2}\sum_{m,I} \left|\langle I|\Lambda_+ \alpha_+ e^{i\mathbf{q}\cdot\mathbf{r}}|0,m\rangle\right|^2 \delta(E_I - E_0 - \nu) \tag{19}$$

where $|0,m\rangle$ is the ground state with spin projection $m = \pm\frac{1}{2}$, $\alpha_+ = \gamma^0\gamma_+$, $\gamma_+ = \frac{1}{\sqrt{2}}(\gamma^1 + i\gamma^2)$, and the $\frac{1}{2}\sum_{m,I}$ averages over initial spins and sums over final states, $|I\rangle$. We assume that the negative energy states are occupied and thus excluded from the sum over final states by

Pauli exclusion. The + superscript on the structure functions indicates this exclusion. The projection operators on positive and negative energy states are defined by

$$\Lambda_+ = \sum_{I, E_I \geq E_0} |I\rangle\langle I| \tag{20}$$

$$\Lambda_- = \sum_{I, E_I < E_0} |I\rangle\langle I|, \tag{21}$$

respectively. The states $|I\rangle$ are orthonormal $\langle I|J\rangle = \delta_{IJ}$. In the interest of subsequent discussion we also define $W^-_{L,T}$ with Λ_- in Eqs.(18) and (19) instead of Λ_+.

The longitudinal and transverse structure functions $W^+_{L,T}$ are related to the response of the electromagnetic probe to the charge and spin fluctuations in the target, respectively. They are viewed as the response of the light, positive energy valence quark in a heavy-light meson, such as $\bar{t}u$, as it is excited into a positive energy final state within the potential well. The longitudinal function W^+_L is associated with a spin-independent coupling of the probe to the target and thus the spin of the struck constituent is unchanged in contributions to it. The transverse function W^+_T is associated with a spin-flip of the struck constituent and couples the upper and lower components of its wave function since

$$\gamma_+ = \begin{pmatrix} 0 & \sqrt{2}\sigma_+ \\ -\sqrt{2}\sigma_+ & 0 \end{pmatrix}, \tag{22}$$

where σ_+ is the raising operator on Pauli spinors.

We calculate the structure functions in a large basis of eigenstates of the Dirac Hamiltonian [Eq.(5)] including values of κ in the range $-100 \leq \kappa < 0$ and $0 < \kappa \leq 100$ in the sum over I in Eqs.(18, 19). We take 400 positive (negative) energy radial states each for each value of κ for the calculation of $W^+(W^-)$. We ensure that this basis supports all the states accessed by scattering up to $|\mathbf{q}| = 12.5$ GeV to a level of 0.3% as measured by the static structure functions, $S_{L,T}(|\mathbf{q}|)$ (as shown below).

In order to obtain the structure functions as smooth curves we fold them with a Breit-Wigner function letting

$$\delta(E_I - E_0 - \nu) \to \frac{\Gamma(\nu)}{2\pi} \frac{1}{(E_I - E_0 - \nu)^2 + \Gamma^2(\nu)/4}, \tag{23}$$

with level width $\Gamma(\nu)$. We use the parameterization for $\Gamma(\nu)$ given in Eq.(8) of Ref.[5] with $\Gamma_0 = 100$ MeV. The effects of hadronization of the excited states are taken into account qualitatively by this prescription.

Figure (1) shows $W_L^+(|\mathbf{q}|,\nu)$ for various values of $|\mathbf{q}|$ plotted as a function of the variable $\tilde{y} = \nu - |\mathbf{q}|$. We note some features of the W_L^+. The curves at high $|\mathbf{q}| \gtrsim 2.5$ GeV, much larger than the characteristic energy scale of $\sigma^{1/4} = 440$ MeV, exhibit scaling in the variable $\tilde{y}$. There is non-zero strength in the timelike region where $\tilde{y} > 0$ corresponding to the fact that the confined constituent is *bound* in the target. The strength in the timelike region for $|\mathbf{q}| = 12.5$ GeV is 7.3% and 11.5% for $\Gamma_0 = 0$ and 100 MeV, respectively. At $|\mathbf{q}| \lesssim 2.5$ GeV the curves exhibit resonances for $\tilde{y} \sim -|\mathbf{q}|$ and show Bloom-Gilman duality.[5, 7] The quality of scaling is fair though scaling violations are significant in the timelike region having $\tilde{y} > 0$ in the present $|\mathbf{q}|$ range. In order to understand these violations we will discuss sum rules.

The full strength of the ground state is distributed among the the positive and negative energy eigenstates by the current $\gamma^\mu e^{i\mathbf{q}\cdot\mathbf{r}}$. Therefore both W_L^+ and W_L^- must be taken into account to support the full strength of the ground state. If we write

$$W_L(|\mathbf{q}|,\nu) = W_L^+(|\mathbf{q}|,\nu) + W_L^-(|\mathbf{q}|,\nu) \tag{24}$$

we obtain a function which satisfies the sum rule

$$S_L(|\mathbf{q}|) = \int_{-\infty}^{\infty} d\nu W_L(|\mathbf{q}|,\nu) = 1, \tag{25}$$

where $S_L(|\mathbf{q}|)$ is the longitudinal static structure function. Here we have integrated over all values of energy transfer ν including the region $\nu < 0$ and used completeness

$$\sum_I |I\rangle\langle I| = 1. \tag{26}$$

(In fact, in our numerical study, $S_L(|\mathbf{q}|)$ has the value of unity to 0.3% or better for all considered $|\mathbf{q}|$.)

The total strength of the $W_L^+(|\mathbf{q}|,\nu)$

$$S_L^+(|\mathbf{q}|) = \int_0^{\infty} W_L^+(|\mathbf{q}|,\nu) < 1 \tag{27}$$

since we have neglected the contribution of the negative energy states. As $|\mathbf{q}|$ increases, the strength $S_L^+(|\mathbf{q}|)$ due to the positive energy states decreases. It can be shown (see Appendix B) that

$$\lim_{|\mathbf{q}|\to\infty} S_L^+(|\mathbf{q}|) = \frac{1}{2}. \tag{28}$$

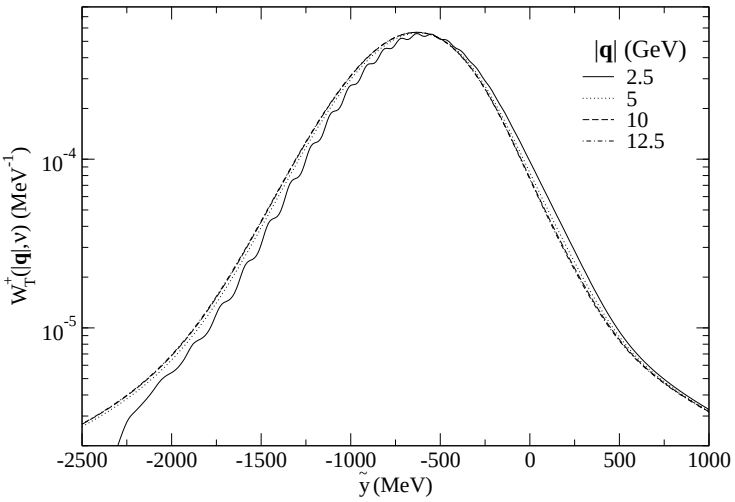

FIG. 2: The transverse structure function $W_T^+(|\mathbf{q}|,\nu)$ vs. $\tilde{y} = \nu - |\mathbf{q}|$ for four values of $|\mathbf{q}| = 2.5, 5, 10, 12.5$ GeV.

At $|\mathbf{q}| = 12.5$ GeV the $S_L^+(|\mathbf{q}|) = 0.52$, independent of Γ_0. The strength missing from $S_L^+(|\mathbf{q}|)$ is taken up by the negative energy states

$$S_L^-(|\mathbf{q}|) = \int_{-\infty}^{0} d\nu W_L^-(|\mathbf{q}|,\nu) \tag{29}$$

to maintain the sum rule Eq.(25). The scaling violations in W_L^+ are due to the sharing of the strength of the ground state between the positive and negative energy eigenstates of the potential.

We expect similar scaling violations in the case of the transverse structure function $W_T^+(|\mathbf{q}|,\nu)$ which we have shown in Fig.(2). The strength in the timelike region for $|\mathbf{q}| = 12.5$ GeV is 1.4% and 4.5% for $\Gamma_0 = 0, 100$ MeV, respectively.

The transverse structure function $W_T(|\mathbf{q}|,\nu)$, defined analogously to Eq.(24), satisfies the sum rule

$$\begin{aligned} S_T(|\mathbf{q}|) &= \int_{-\infty}^{\infty} d\nu W_T(|\mathbf{q}|,\nu) \qquad (30) \\ &= \frac{1}{2}\sum_m \langle 0,m|(1-\sigma_z)|0,m\rangle \\ &= \frac{5}{6} + \frac{1}{6} = 1, \qquad (31) \end{aligned}$$

where the first and second terms in Eq.(31) correspond to $m = -\frac{1}{2}$ and $m = +\frac{1}{2}$, respectively. The different strengths in $m = \pm\frac{1}{2}$ can be understood by analyzing the ground state wave

function. The matrix operator α_+ in Eq.(19) corresponds to a virtual photon with positive helicity and therefore can only scatter from components of the wave function which have Pauli-spin down. The ground state wave function is s-wave in the upper component and the photon can't scatter from it when $m = +\frac{1}{2}$. It only scatters from the spin down part of the p-wave lower component resulting in less strength for the $m = +\frac{1}{2}$ state than in the $m = -\frac{1}{2}$ state.

In deriving the result Eq.(31) we used the facts that

$$\int_0^\infty dr\ r^2 f_0^2(r) = \frac{3}{4} \tag{32}$$

$$\int_0^\infty dr\ r^2 g_0^2(r) = \frac{1}{4} \tag{33}$$

where $rf_0(r)$ and $rg_0(r)$ are the upper and lower radial wave functions for the ground state. These follow directly from the Dirac equation for a massless constituent independent of the string tension $\sqrt{\sigma}$ as illustrated in Appendix C. Additionally it can be shown that

$$E_0 = 2\langle V\rangle_0, \tag{34}$$

where $\langle O\rangle_0 \equiv \int d^3r \Psi_0^\dagger(\mathbf{r}) O \Psi_0(\mathbf{r})$.

Up to this point we have calculated the structure functions $W_{L,T}^+$ for a confined Dirac valence particle. These functions concern the scattering of the valence particle in the ground state to a positive energy excited state. The contribution of the negative energy states in the sum over intermediate states I in Eq.(18) has been ignored since these states are assumed to be filled.

We now consider the response of the vacuum in the presence of the infinitely massive color source. The response of the vacuum corresponds to scattering from a negative energy state into a positive energy state. Consider the contribution to the vacuum response when the particle is initially in a negative energy state I and scatters into the unoccupied ground state:

$$W_L^{(0)-}(|\mathbf{q}|,\nu) = \frac{1}{2}\sum_{m,I} |\langle 0,m|e^{-i\mathbf{q}\cdot\mathbf{r}}\Lambda_-|I\rangle|^2 \delta(E_I - E_0 + \nu). \tag{35}$$

Here the superscript $(0)-$ indicates that we are scattering from a negative energy state into the ground state. We have taken the energy transfer $\nu \to -\nu$ since a negative energy state is equivalent to a positive energy antiparticle. This contribution is shown Fig.(3) as a function of $\tilde{y}$ for $|\mathbf{q}| = 10$ GeV. We noted above that the negative energy states depend on

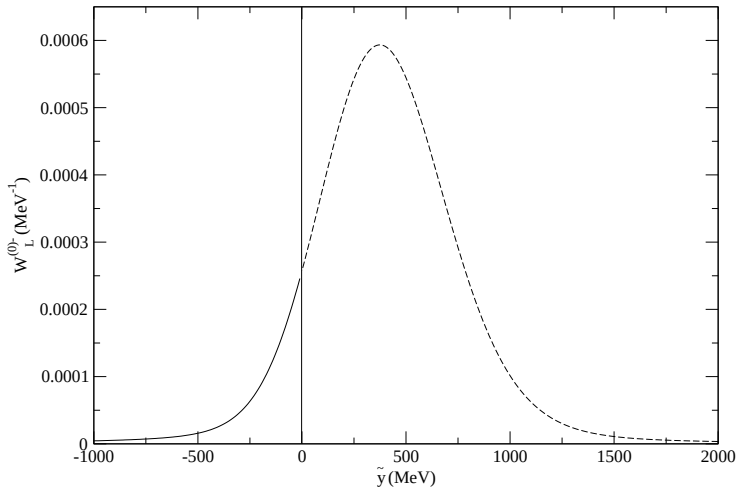

FIG. 3: The vacuum contribution to the longitudinal structure function $W_L^{(0)-}(|\mathbf{q}|,\nu)$ for scattering from a negative energy state into the ground state vs. $\tilde{y} = \nu - |\mathbf{q}|$ for $|\mathbf{q}| = 10$ GeV. Only the solid curve in the region $\tilde{y} < 0$ is physical. The continuation (dashed curve) into the region $\tilde{y} > 0$ has no meaning.

the cavity radius, R, since they are not bound by the potential Eq.(3). However $W_L^{(0)-}$ is only weakly dependent on the cavity radius since the matrix element receives contributions for $r \lesssim 1$ fm, the radial extent of the ground state. At these radii the negative energy states are not sensitive to the boundary condition. This was verified for $R = 10$ and 15 fm. We interpret $W_L^{(0)-}$ as the contribution to the vacuum response in the spacelike $\tilde{y} < 0$ region. It is a consequence of the fact that interactions move some of the strength of the vacuum response from the timelike region into the spacelike region. We cannot reliably calculate the response in the timelike region since confinement acts at all distances in our model. Additional contributions to the vacuum response in the spacelike region correspond to scattering from a negative energy state into a positive energy state J and are denoted $W_L^{(J)-}$. These contributions are smaller than the $W_L^{(0)-}$ since the first excited state has energy $E_{J=1} = 1100$ MeV, 260 MeV above the ground state.

IV. PLANE WAVE IMPULSE APPROXIMATION

We may compare the exact structure functions calculated in the previous section with those obtained in PWIA. We consider only the longitudinal structure function in this section.

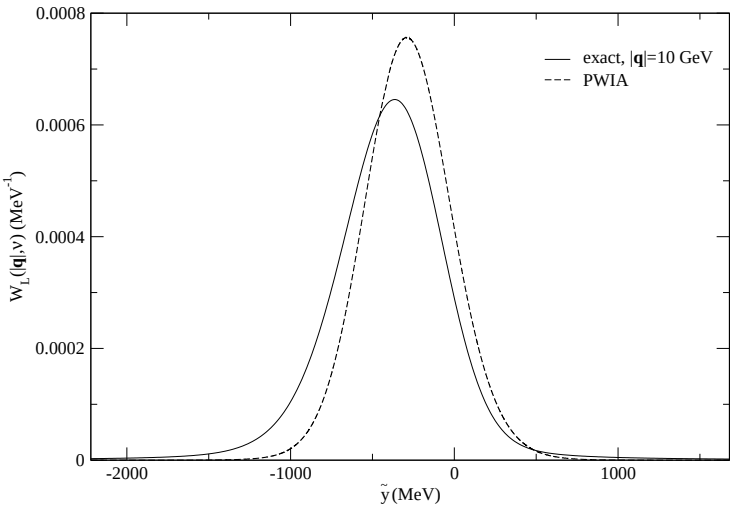

FIG. 4: The longitudinal structure function $W_L^+(|\mathbf{q}|,\nu)$ vs. $\tilde{y} = \nu - |\mathbf{q}|$ in PWIA and the exact result for $|\mathbf{q}| = 10$ GeV.

In PWIA, one assumes that the state of the struck constituent may be described as a plane wave with energy

$$E_{\mathbf{k}+\mathbf{q}} = |\mathbf{k}+\mathbf{q}| + \langle V\rangle_0, \tag{36}$$

for a massless constituent. The expectation value of the potential [Eq.(3)] in the ground state, $\langle V\rangle_0$ is required to give the correct value for the energy weighted sum rule

$$S_L^{(1)+}(|\mathbf{q}|) = \int_0^\infty d\nu\, \nu W_L^+(|\mathbf{q}|,\nu). \tag{37}$$

We may calculate this quantity analytically in the limit $|\mathbf{q}| \to \infty$ using the technique in Appendix B to obtain

$$\lim_{|\mathbf{q}|\to\infty} S_L^{(1)+}(|\mathbf{q}|) = \frac{|\mathbf{q}|}{2}. \tag{38}$$

The PWIA neglects interactions of the struck constituent in the final state. The expression Eq.(18), for example, then simplifies to

$$W^+_{L,PWIA}(|\mathbf{q}|,\nu) = \frac{1}{2}\sum_{s,m}\int \frac{d^3k}{(2\pi)^3}\left|\langle u_{\mathbf{k}+\mathbf{q},s}|e^{i\mathbf{q}\cdot\mathbf{r}}|0,m\rangle\right|^2 \delta(|\mathbf{k}+\mathbf{q}| + \langle V\rangle_0 - E_0 - \nu), \tag{39}$$

where $|u_{\mathbf{k}+\mathbf{q},s}\rangle$ is the positive energy free-particle Dirac spinor with spin s. An analogous expression holds for the $W^+_{T,PWIA}$.

Evaluating the matrix elements in the above equation gives

$$\begin{aligned} W^+_{L,PWIA}(\tilde{y}) \;&=\; \frac{1}{2}\int \frac{d^3k}{4\pi}\left[\tilde{f}_0^2(k) + \tilde{g}_0^2(k) - 2\tilde{f}_0(k)\tilde{g}_0(k)\frac{k_z}{k}\right] \\ &\times\; \delta(k_z - \tilde{y} + \langle V\rangle_0 - E_0), \end{aligned} \tag{40}$$

where we have neglected terms $\mathcal{O}(\frac{1}{|\mathbf{q}|})$ and $\tilde{f}_0(k)$, $\tilde{g}_0(k)$ are the Fourier-Bessel transforms of the radial wave functions appearing in the Fourier transform of the ground state:

$$\tilde{\Psi}_{0,m}(\mathbf{k}) = (2\pi)^{\frac{3}{2}} \begin{pmatrix} \tilde{f}_0(k)\mathcal{Y}^0_{\frac{1}{2},m}(\hat{\mathbf{k}}) \\ \tilde{g}_0(k)\mathcal{Y}^1_{\frac{1}{2},m}(\hat{\mathbf{k}}) \end{pmatrix}. \tag{41}$$

The $\mathcal{Y}^\ell_{jm}$ are the spin-angle functions. Figure 4 shows the PWIA approximation for the longitudinal structure function and the exact result.

The argument of the δ function depends only on the variable $\tilde{y}$ and therefore the PWIA response also exhibits scaling behavior. It has scaling violations which are $\mathcal{O}(\frac{1}{|\mathbf{q}|})$ for $|\mathbf{q}|$ finite. The $W^+_{L,PWIA}$ satisfies the sum rules Eq.(28) and Eq.(37) but has a different shape than the exact curve. It has more response in the timelike region than the exact result with 14.7% of the total strength in the timelike region compared with 11.5% for the exact result. This is a consequence of the interference of the upper and lower components of the ground state wave function in the third term in square brackets of Eq.(40). Neglecting this term, the $W^+_{L,PWIA}$ would peak at $\tilde{y} = -\frac{E_0}{2}$, nearly coincident with the peak of the exact curve. The interference term shifts strength into the timelike region. In a subsequent work we shall explore the consequences of such effects on spin-dependent observables such as the helicity structure function.[1] We note finally that the PWIA and exact curves in Fig.(4) have different widths. The larger width of the exact curve is due to FSI of the struck constituent with the potential, V. As in the case of the semirelativistic model [5], FSI effects persist in the limit $|\mathbf{q}| \to \infty$. We note that Brodsky and collaborators have shown that FSI affect the interpretation of parton distribution functions [9] and can contribute to large single spin asymmetries in semi-inclusive DIS processes [10].

V. CONCLUSION

We have calculated exactly the eigenstates of a massless Dirac particle confined in a linear potential for excitation energies up to ~ 10 GeV. The unpolarized valence quark structure functions of the particle in the ground state scattering into a positive energy excited state were determined by coupling a spin-$\frac{1}{2}$ electromagnetic probe to the conserved vector current of particles in the potential well. The structure functions exhibit $\tilde{y}$ or Nachtmann scaling, a generalization of Bjorken scaling. The exact response takes account of interactions of

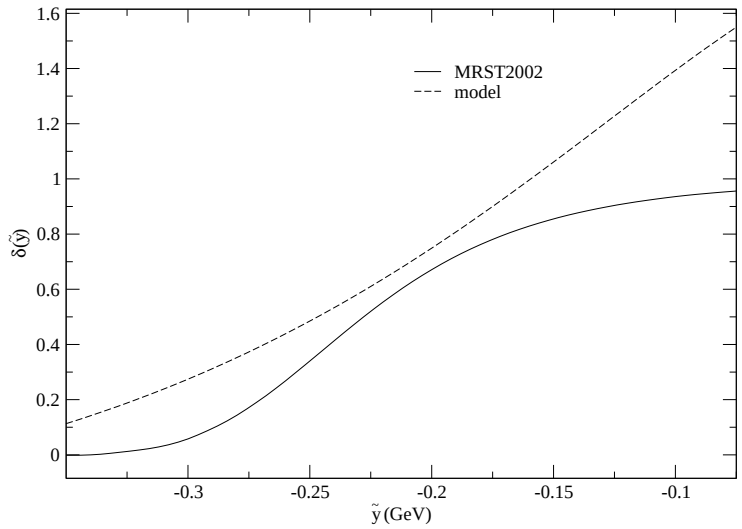

FIG. 5: The deviation from Callan-Gross relation in terms of the function δ of Eq.(42) for $|\mathbf{q}| = 10$ GeV. The dashed curve is the scaled model calculation (see text). The solid curve is the MRST2002 *pdf* fit to data.

the confined particle both before and after interaction with the electromagnetic probe and therefore $\tilde{y}$ or Bjorken scaling is not a consequence of treating the constituent of the target as a free particle. In contrast to Refs.[11, 12] who find that FSI have no effect on the structure functions, and therefore also conclude that Bjorken scaling applies to systems of interacting constituents, the present model does not reproduce the parton model results when FSI are taken into account.

Another example of the role interactions have in determining the structure function of confined Dirac particles can be seen if we consider the function

$$\delta(\tilde{y}, |\mathbf{q}|) = \frac{F_2(\tilde{y}, |\mathbf{q}|) - 2xF_1(\tilde{y}, |\mathbf{q}|)}{F_2(\tilde{y}, |\mathbf{q}|) + 2xF_1(\tilde{y}, |\mathbf{q}|)} \tag{42}$$

where $F_1 = MW_1$ and $F_2 = \nu W_2$, M is the mass of the target. At leading order in the quark-parton model one obtains $\delta(\tilde{y}, |\mathbf{q}|) = 0$ (the Callan-Gross relation [13]) for all $\tilde{y}$ and $|\mathbf{q}|$. In Fig.(5) we have plotted, for $|\mathbf{q}| = 10$ GeV, the MRST2002 [14] fit (solid curve) to deep inelastic data using the next-to leading order prediction [15]

$$F_L(x, Q^2) = \frac{2.5}{5.9}\frac{4\pi}{\alpha_s(Q^2)} x g(2.5x, Q^2), \tag{43}$$

where $0 < x < 0.4$ and $g(x, Q^2)$ is the prediction for the gluon. It is compared to the present model calculation (dashed curve) which has been rescaled in order to obtain agreement with

the first moment of the *up* valence quark distribution for the MRST *pdf* assuming that the response of the proton is due to a single *up* valence quark. The non-perturbative effects of interactions could be the origin of the difference in the two curves in Fig.(5).

In future work we will apply the present model to the study of spin-dependent effects such as the helicity and transversity distribution of the constituents of the target. We expect that these observables depend strongly upon the relativistic treatment of the constituent as a Dirac particle. The comparison of the present model with experimental data requires one to include radiative gluon effects to obtain the Q^2 evolution of the structure functions. This problem is currently under study.

APPENDIX A: BAG MODEL BASIS STATES

The free Dirac Hamiltonian H_0 is

$$\begin{aligned}\left[\boldsymbol{\alpha}\cdot\mathbf{p}+\beta m\right]\Phi^P_{\alpha\kappa m} &= \mathrm{sgn}P\sqrt{(p_{\alpha\kappa})^2+m^2}\,\Phi^P_{\alpha\kappa m}\\ &= \mathrm{sgn}P E_{\alpha\kappa}\Phi^P_{\alpha\kappa m},\end{aligned}\tag{A1}$$

for a particle of mass m (not to be confused with the total spin projection which appears as the subscript m in the wave function $\Phi^P_{\alpha\kappa m}$). The complete set of states includes states of positive $E_{\alpha\kappa}>0$ energy states, 'particles' and negative $E_{\alpha\kappa}<0$ energy states, 'antiparticles.' The bag model states are solutions of Eq.(A1) within a cavity of radius R. These particle states may be written as

$$\Phi^+_{\alpha\kappa m}(\mathbf{r}) = N_{\alpha\kappa}\begin{pmatrix} j_\ell(p_{\alpha\kappa}r)\mathcal{Y}^\ell_{jm}\\ -i\sqrt{\frac{E_{\alpha\kappa}-m}{E_{\alpha\kappa}+m}}j_{\ell+1}(p_{\alpha\kappa}r)\mathcal{Y}^{\ell+1}_{jm}\end{pmatrix},\kappa<0\tag{A2}$$

$$\Phi^+_{\alpha\kappa m}(\mathbf{r}) = N_{\alpha\kappa}\begin{pmatrix} j_\ell(p_{\alpha\kappa}r)\mathcal{Y}^\ell_{jm}\\ i\sqrt{\frac{E_{\alpha\kappa}-m}{E_{\alpha\kappa}+m}}j_{\ell-1}(p_{\alpha\kappa}r)\mathcal{Y}^{\ell-1}_{jm}\end{pmatrix},\kappa>0.\tag{A3}$$

Here the normalization $N_{\alpha\kappa}$ is fixed by the condition $\int d^3r\Phi^{+\dagger}_{\alpha\kappa m}(\mathbf{r})\Phi^+_{\alpha\kappa m}(\mathbf{r})=1$ to give

$$N_{\alpha\kappa}=\left\{R^3\left[\frac{2(E_{\alpha\kappa})^2}{(p_{\alpha\kappa})^2}+\frac{1}{(p_{\alpha\kappa})^2R}(m+2E_{\alpha\kappa}\kappa)\right]j^2_{\pm(\kappa+1)}(p_{\alpha\kappa}R)\right\}^{-\frac{1}{2}}.\tag{A4}$$

The upper (lower) sign corresponds to κ positive (negative).

The antiparticle (negative energy) states are obtained from Eqs.(A2) and (A3) by interchanging upper and lower components and multiplying one of them by -1. With this

prescription the sign of κ for the negative energy state is opposite to the sign of κ of the positive energy state from which it was obtained.

As mentioned in the text, we determine the allowed $p_{\kappa\alpha}$ by subjecting the $\Phi_{\alpha\kappa m}$ to the bag model boundary condition at $r = R$

$$\overline{\Phi}\Phi\big|_{r=R} = 0, \tag{A5}$$

where $\overline{\Phi} = \Phi^\dagger\beta$. Substitution of the wave functions in Eqs.(A2) and (A3) into this expression results in the following transcendental equations; for $\kappa = -(\ell+1) < 0$

$$j_\ell(p_{\alpha\kappa}R) = \sqrt{\frac{E_{\alpha\kappa}-m}{E_{\alpha\kappa}+m}}\, j_{\ell+1}(p_{\alpha\kappa}R), \tag{A6}$$

and for $\kappa = \ell > 0$

$$j_\ell(p_{\alpha\kappa}R) = -\sqrt{\frac{E_{\alpha\kappa}-m}{E_{\alpha\kappa}+m}}\, j_{\ell-1}(p_{\alpha\kappa}R). \tag{A7}$$

The subscript $\alpha = 1, \ldots, \infty$ indexes the solutions of the transcendental equations. The number of nodes in the upper component radial function is $(\alpha - 1)$.

APPENDIX B: $S_L^+(|\mathbf{q}|)$ IN THE LIMIT $|\mathbf{q}| \to \infty$

The expression for the $S_L^+(|\mathbf{q}|)$ is given by

$$S_L^+(|\mathbf{q}|) = \int_0^\infty d\nu W_L^+(|\mathbf{q}|) \tag{B1}$$

$$= \frac{1}{2}\sum_m \langle 0,m|e^{-i\mathbf{q}\cdot\mathbf{r}}\Lambda_+ e^{i\mathbf{q}\cdot\mathbf{r}}|0,m\rangle. \tag{B2}$$

We may evaluate this expression analytically in the limit $|\mathbf{q}| \to \infty$ by recognizing that in this limit the intermediate states $|I\rangle$ in Eq.(B2) may be taken to be free-particle solutions, $|u_{\mathbf{k}+\mathbf{q},s}\rangle$ of the Dirac equation since their overlap with the ground state is dominated by small radii $\lesssim 1$ fm where the exact wave functions resemble free-particle wave functions. Thus we replace

$$e^{-i\mathbf{q}\cdot\mathbf{r}}\Lambda_+ e^{i\mathbf{q}\cdot\mathbf{r}} \to e^{-i\mathbf{q}\cdot\mathbf{r}}\sum_s \int \frac{d^3k}{(2\pi)^3}|u_{\mathbf{k}+\mathbf{q}},s\rangle\langle u_{\mathbf{k}+\mathbf{q}},s|e^{i\mathbf{q}\cdot\mathbf{r}}, \tag{B3}$$

valid in the limit $|\mathbf{q}| \to \infty$ and obtain upon substitution into Eq.(B2)

$$S_L^+(|\mathbf{q}|) = \frac{1}{2}\sum_m \int \frac{d^3k}{(2\pi)^3}\Psi_{0,m}^\dagger(\mathbf{k})\sum_s u_{\mathbf{k}+\mathbf{q},s}u_{\mathbf{k}+\mathbf{q},s}^\dagger\Psi_{0,m}(\mathbf{k}). \tag{B4}$$

The projection operator for free-particle solutions to the Dirac equation, expressed to $\mathcal{O}\left(\frac{1}{|\mathbf{q}|}\right)$, is

$$\sum_s u_{\mathbf{k}+\mathbf{q},s} u^\dagger_{\mathbf{k}+\mathbf{q},s} = \frac{1}{2}\left(1 + \alpha_z + \frac{\boldsymbol{\alpha}\cdot\mathbf{k}_\perp}{|\mathbf{q}|}\right), \tag{B5}$$

where $\mathbf{q} = |\mathbf{q}|\hat{\mathbf{z}}$ and $\mathbf{k}_\perp = (k_x, k_y)$. Substitution of Eq.(B5) into Eq.(B4) gives the result Eq.(28).

APPENDIX C: GROUND STATE NORMALIZATIONS

The Dirac equation for the ground state gives

$$f_0'(r) = E_0 g_0(r) \tag{C1}$$

$$-g_0'(r) - \frac{2}{r} g_0(r) = (E_0 - \sqrt{\sigma} r) f_0(r). \tag{C2}$$

for the upper and lower radial wave functions. Multiplying Eq.(C1) by $g_0(r)$ and Eq.(C2) by $f_0(r)$, summing and integrating gives

$$E_0 \int_0^\infty dr r^2 (f_0^2(r) - g_0^2(r)) = \sqrt{\sigma} \int_0^\infty dr r^2 f_0^2(r) r. \tag{C3}$$

The r.h.s. of the above is the expectation value of the potential $V(r) = \sqrt{\sigma} r(1+\beta)$ in the ground state since it doesn't couple to the lower components of the wave function. Substitute Eq.(34) into Eq.(C3) to obtain

$$\int_0^\infty dr r^2 (f_0^2(r) - g_0^2(r)) = \frac{1}{2}. \tag{C4}$$

The normalization condition is:

$$\int_0^\infty dr r^2 (f_0^2(r) + g_0^2(r)) = 1. \tag{C5}$$

Adding and subtracting these equations gives the result Eqs.(32), independent of the string tension, $\sqrt{\sigma}$.

ACKNOWLEDGMENTS

The author wishes to thank the *Schweizerische Nationalfonds* for support and Omar Benhar, Joseph Carlson, Vijay Pandharipande, and Ingo Sick for many useful discussions.

This work has been supported by U.S. Department of Energy under contract W-7405-ENG-36.

---

[1] V. R. Pandharipande, M. W. Paris, and I. Sick (2003), in preparation.

[2] O. Benhar, V. R. Pandharipande, and I. Sick, Phys. Lett. **B489**, 131 (2000).

[3] O. Nachtmann, Nucl. Phys. B **63**, 237 (1973).

[4] M. W. Paris and V. R. Pandharipande, Phys. Rev. C **65**, 035203 (2002).

[5] M. W. Paris and V. R. Pandharipande, Phys. Lett. **B514**, 361 (2001).

[6] I. Niculescu et al., Phys. Rev. Lett. **85**, 1182 (2000).

[7] E. Bloom and F. Gilman, Phys. Rev. Lett. **25**, 1140 (1970).

[8] P. R. Page, T. Goldman, and J. N. Ginocchio, Phys. Rev. Lett. **86**, 204 (2001), hep-ph/0002094.

[9] S. J. Brodsky, P. Hoyer, N. Marchal, S. Peigne, and F. Sannino, Phys. Rev. D **65**, 114025 (2002).

[10] S. J. Brodsky, D. S. Hwang, and I. Schmidt, Int. J. Mod. Phys. **A18**, 1327 (2003).

[11] E. Pace, G. Salme, and F. M. Lev, Phys. Rev. C **57**, 2655 (1998).

[12] S. Jeschonnek and J. W. Van Orden, Phys. Rev. **D65**, 094038 (2002), hep-ph/0201113.

[13] C. Callan and D. J. Gross, Phys. Rev. Lett. **22**, 156 (1969).

[14] A. D. Martin, R. G. Roberts, W. J. Stirling, and R. S. Thorne (2002), hep-ph/0211080.

[15] A. M. Cooper-Sarkar, G. Ingelman, K. R. Long, R. G. Roberts, and D. H. Saxon, Z. Phys. **C39**, 281 (1988).